Gene Microarray Analysis of Experimental Glaucomatous Retina from Cynomologous Monkey

Teruyoshi Miyahara,[1] *Takanobu Kikuchi,*[2] *Masayuki Akimoto,*[1] *Toru Kurokawa,*[1] *Hiroto Shibuki,*[1] *and Nagahisa Yoshimura*[1]

Purpose. To systematically explore changes in gene expression in the retina of monkeys with laser-induced glaucoma and to validate the microarray data on eyes with experimental glaucoma.

Methods. Glaucoma was induced in the right eye of four monkeys by repeated argon laser photocoagulation of the trabecular meshwork. The left eye served as the control. Retinas were isolated from glaucomatous and control eyes 30 days after photocoagulation. Gene expression changes were analyzed by human microarray chips which displayed a total of 9182 elements including Expression Sequence Tag (EST) clones. Changes in the expression of some genes were further confirmed by real-time PCR analysis. Immunohistochemical studies to examine protein expression of some gene products were also done for several genes that showed up- or downregulation by the microarray analysis.

Results. Two eyes with mild glaucoma and two with severe glaucoma were produced. In the mild and severe glaucomatous retina, the number of upregulated genes was 45 and 18, and the number of downregulated genes was 17 and 21, respectively. The number of genes that were up- or downregulated was 0.7% of all the genes examined. The real-time PCR analysis confirmed expression changes of some genes found in the microarray analysis. Ceruloplasmin was one of the upregulated genes, and it was found by immunohistochemical analyses to be expressed in Müller cells.

Conclusions. Gene expression profiles in laser-induced glaucomatous monkey retinas were determined, and only a very small population of genes was up- or downregulated in glaucomatous eyes. Upregulation of ceruloplasmin protein was found in the Müller cells. (*Invest Ophthalmol Vis Sci.* 2003;44: 4347–4356) DOI:10.1167/iovs.02-1032

Glaucoma is one of the most important eye diseases and the leading cause of blindness in the developed countries.[1] In glaucomatous eyes, there is progressive optic nerve damage with selective loss of the retinal ganglion cells (RGCs). The precise mechanism for the RGC loss in glaucomatous eyes has yet to be determined, but it is widely accepted that apoptosis plays an important role.[2,3]

Deficient growth factors, glutamate toxicity, and abnormal nitric oxide metabolism have been proposed as possible factors that trigger RGC apoptosis.[4–9] In apoptosis, de novo gene expression is known to be important in the execution step.[10] However, to the best of our knowledge, no report has been published on systematic studies of gene expression changes in the glaucomatous retina. Such a report is important because a systematic profiling of the gene expression changes in glaucomatous eyes will give us important information on the mechanism of RGC death in the disease and may provide us with new therapeutic tools.

Although the occurrence of normal tension glaucoma is well known, it is widely accepted that high IOP is a consistent risk factor in glaucoma. Many rat models of glaucoma with high IOP have been reported, and such convenient and nonexpensive experimental models are widely used to study the pathogenesis of glaucomatous neuronal damage.[11–14] A laser-induced glaucoma model in monkeys is much more difficult to produce, and extensive studies to profile gene expression changes in such models are not easily accomplished. However, such a primate model is important because it mimics human ocular hypertension glaucoma in many respects.[15,16]

Recently, microarray technology has rapidly developed[17–20] and we can now use the technology for various studies. In this report, we systematically studied gene expression changes in the retinas of monkeys with laser-induced glaucoma using the microarray technology.

Materials and Methods

Glaucoma Model

Four cynomolgus monkeys (monkeys #1 to #4) were used: monkeys #1 and #2 were used for the microarray analyses, and monkeys #3 and #4 for immunohistochemical studies. The monkeys received a baseline examination including slit-lamp examination, measurement of the IOP, and gonioscopy with a goniolens. In addition, the fundus were examined and photographed with a fundus camera (Topcon, Tokyo, Japan) after topical phenylephrine and tropicamide mydriasis. The IOP was measured with a pneumatonometer (Alcon, Fort Worth, TX). At the beginning, eyes had normal anterior segments, optic nerve heads, and IOPs (normal range, 20–25 mm Hg).

Glaucoma was induced in the right eye of the four monkeys by repeated argon laser photocoagulation of the trabecular meshwork as previously described.[21,22] The fellow eyes were used as the control. Animals were anesthetized with ketamine hydrochloride (5 mg/kg intramuscularly, supplemented with 2.5 mg/kg intramuscularly as needed) and sedated with xylazine (0.25 mg/kg intramuscularly). The eyes of the monkeys were examined at least once a week after the laser treatment. The examination includes slit-lamp biomicroscopy to check for corneal clarity, cells in the anterior chamber, and flare. After measurements of the IOP, the anterior chamber angle was examined with a goniolens. The pupil was dilated by topical phenylephrine and tropicamide, and the optic nerve heads were examined and fundus photographs were taken.

Thirty days after the laser treatment, monkeys #1 and #2 were deeply anesthetized with a mixture of ketamine hydrochloride (7.5 mg/kg) and xylazine (0.5 mg/kg) intramuscularly and were killed by

From the [1]Department of Ophthalmology, and the [2]Research Center for Instrumental Analysis, Shinshu University School of Medicine, Matsumoto, Japan.

Supported in part by Grants-in-Aid (13470364 and 14770950) from the Ministry of Education, Culture, Sports, Science and Technology of the Japanese Government.

Submitted for publication October 8, 2002; revised April 10 and May 28, 2003; accepted May 29, 2003.

Disclosure: **T. Miyahara**, None; **T. Kikuchi**, None; **M. Akimoto**, None; **T. Kurokawa**, None; **H. Shibuki**, None; **N. Yoshimura**, None

The publication costs of this article were defrayed in part by page charge payment. This article must therefore be marked "*advertisement*" in accordance with 18 U.S.C. §1734 solely to indicate this fact.

Corresponding author: Nagahisa Yoshimura, Department of Ophthalmology, Shinshu University School of Medicine, Matsumoto 390–8621, Japan; nagaeye@hsp.md.shinshu-u.ac.jp.

Table 1. Primer and Probe Sequences Used for the Real-Time PCR Analysis

Gene	Primers for PCR and Sequence Analysis (5′ to 3′)	Primers for Real-Time PCR (5′ to 3′)	TaqMan Probe (5′ to 3′)
AKT1			
Forward	CTCACCCAGTGACAACTCAG	GAGGTGTCCCTGGCCAAAC	FAM-AACGAGTTTGAGTACCTGAA-MGB
Reverse	TTCCTTCTTGAGGATCTTCATG	CCTTCTCCTTCACCAGGATCAC	
chitinase 3-like 1			
Forward	TCAAACAGGCTTTGTGGTCC	TCCAGTGCTGCTCTGCATACA	FAM-ACTGGTCTGCTACTACAC-MGB
Reverse	GTCACATCATTCCACTCCCA	AAGCGGTCAATGGCATCTG	
GFAP			
Forward	AGCCTCAAGGACGAGATGG	GATCGCCACCTACAGGAAGCT	FAM-AGGAGAACCGGATCAC-MGB
Reverse	CACGATGTTCCTCTTGAGGT	TGGAGAAGGTCTGCACAGGAA	
ceruloplasmin			
Forward	TTGATGAGAATGAATCTTGGTACT	GATGATGAGGAATTCATAGAAAGCA	FAM-AAATGCATGCTATTAATGG-MGB
Reverse	TCACATGGCAGTGGAGTAAC	TGAGGCCTTGTAGGTTTCCAA	
*β-actin**			

* The sequence is not provided by the manufacturer (catalog #4333762; PE Biosystems, Foster City, CA).

intravenous thiopental sodium (100 mg/kg). For the imunohistochemical studies, Monkeys #3 and #4 were given an overdose of ketamine hydrochloride and xylazine and immediately killed by exsanguination. They were perfused with heparinized normal saline solution followed by 4% paraformaldehyde. The eyes were then carefully enucleated and were further immersed in the same fixative overnight before paraffin embedding. Specimens for microarray were handled using sterile techniques to avoid RNase contamination. Evidence of glaucomatous disc cupping by funduscopic examination determined the day monkeys were killed.

All experiments were performed in compliance with the ARVO Statement for the Use of Animals in Ophthalmic and Vision Research.

Microarray Analysis

Poly(A) mRNA was isolated from the monkey retinas with an mRNA isolation kit (FastTrack 2.0; Invitrogen, Carlsbad, CA). Isolated mRNA (200 ng) was reverse transcribed with 5′Cy3- or Cy5-labeled random 9-mers (Operon Technologies, Inc., Alameda, CA) and Moloney Murine Leukemia Virus (MMLV) reverse transcriptase (Life Technologies, Gaithersburg, MD). The Cy3-labeled 9-mer was used for probe 1 (control retina), and the Cy5-labeled 9-mer for probe 2 (laser-induced glaucomatous retina).

The labeled probe pairs were used for microarray hybridization to a human chip (UniGEM Human V ver.2.0; Incyte Genomics, Palo Alto, CA) containing 9182 human cDNA elements. The specifically bound probes on the microarray were scanned for the two individual fluorescent colors, and the signals were corrected and normalized for the differences between the Cy3 and Cy5 channels. The ratio of the two normalized probe signals provided a quantitative measurement of the relative level of gene expression in the glaucomatous retina relative to the control retina.

Real-Time PCR Analysis

Because the cDNA sequences for the target monkey genes are not available, PCR were performed on monkey retinal cDNA generated from the reverse transcriptase reaction using primers designed on conserved regions of genes of several animal species. The PCR products were isolated by agarose gel electrophoresis and were directly sequenced by an autosequencer (ABI PRISM 3100PE; Biosystems, Foster City, CA). The monkey cDNA sequences thus obtained were then used to design TaqMan primer and probe sets for the real-time PCR assay (Primer Express software; PE Biosystems, Foster City, CA). The TaqMan probes were labeled with the 5′ reporter dye FAM and the 3′ nonfluorescent quencher with minor grove binder. Table 1 summarizes all the primer and probe sequences used in this study. Four sets of primers and probes were designed from monkey cDNA sequences to study mRNA expression changes in the severe glaucoma retina (monkey #2, right eye) and the control retina (monkey #2, left eye). The genes studied include ceruloplasmin, GFAP, chitinase-3 like 1, and akt-1. The mRNA in microarray analysis was used for the real-time PCR analysis. First-strand cDNA was synthesized from 200 ng of mRNA with oligo(dN)$_6$ (Amersham Biosciences, Uppsala, Sweden) in a total volume of 33 μL aliquots of cDNA target template diluted serially and mixed with 900 nM of primers and 200 nM of TaqMan probe. The reactions were carried out in a master mix (Universal PCR; PE Biosystems), containing $MgCl_2$, dNTP, and DNA polymerase AmpliTaq Gold in a total volume of 50 μL The PCR reactions were carrried out in duplicates on an ABI PRISM 7000 Sequence detection system (PE Biosystems). The reaction program was as follows: the initial step of 2 minutes at 50°C; denaturation at 95°C for 10 minutes, followed by 45 thermal cycles of denaturation (15 seconds at 95°C) and elongation (1 minute at 60°C). The relative quantitation of the target mRNAs was carried out using the comparative method.[23] The mRNA expression levels for all samples were normalized to the levels for the housekeeping gene β–actin.

Immunohistochemistry

Sections of eyes (4-μm thick) of monkeys #3 and #4 were blocked with 1% BSA for 30 minutes at room temperature. The sections were rinsed with PBS and were then incubated overnight at 4°C with rabbit polyclonal anticeruloplasmin antibody (1:100; Nordic Immunologic Laboratories, Tilburg, The Netherlands), mouse monoclonal antiglial fibrillary acidic protein antibody (GFAP) (1:100; Chemicon International, Temecula, CA), goat polyclonal anti-akt1 antibody (1:50; Santa Cruz Biotechnology, Santa Cruz, CA), rabbit polyclonal antineurofilament 200 kDa antibody (1:200; Chemicon International), or mouse monoclonal antiparvalbumin antibody (1:100; Sigma, St Louis, MO). The working concentrations of the antibodies were determined after various concentrations were tested. After rinsing, FITC-conjugated second antibodies (1:30; Dako, Glostrup, Denmark) or Alexa fluor 488-conjugated second antibodies (1:100; Molecular Probes, Leiden, The Netherlands) were used to obtain green fluorescence. The nuclei were then counterstained with propidium iodide (20 μg/mL).[24,25]

Double immunostaining for ceruloplasmin and GFAP was performed on retinal sections of the right eye of monkey #3 (severe glaucoma). The sections were incubated in a mixture of mouse monoclonal anti-GFAP antibody (1:100) and rabbit anticeruloplasmin antibody (1:100) overnight at 4°C. The sections were then rinsed and incubated with FITC-conjugated antimouse IgG (1:30) and Cy3-conjugated antirabbit IgG (1:30).[24,25] To study glaucomatous changes, longitudinal sections of the optic disc were obtained from the left eye of monkey #1 and both eyes of monkeys #3 and #4, and hematoxylin-eosin (HE) staining was performed.

All immumnohistochemical specimens were examined with a scanning laser confocal microscope (LSM410; Carl Zeiss, Oberkochen, Germany) under the fluorescence mode and HE-stained sections were observed by a light microscope.

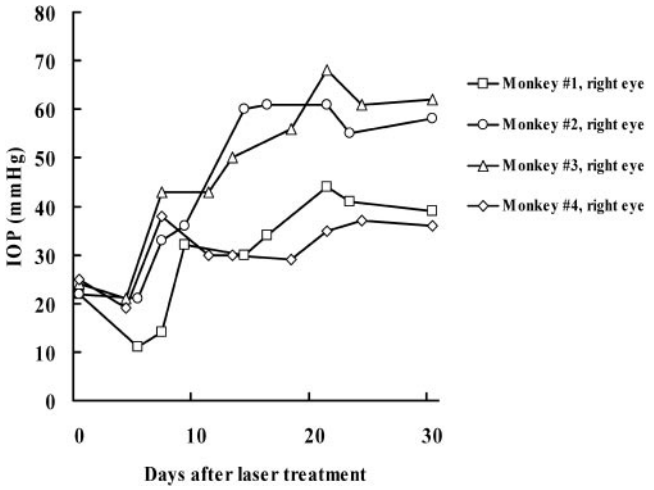

FIGURE 1. IOP changes after the laser treatment. The IOP shows a rise 7 to 10 days after the laser delivery. The IOPs in monkeys #2 and #3 increased to >50 mm Hg whereas that in monkeys #1 and #4 increased to ~40 mm Hg at their peak.

RESULTS

Changes of IOP and Optic Nerve

The IOP of the laser-treated eyes increased to >35 mm Hg, although some fluctuations were found. The rise in the IOP was detected in 7 to 10 days after the laser treatment (Fig. 1). In monkeys #1 and #4, the IOP remained between 30 to 40 mm Hg for approximately 20 days. In monkeys #2 and #3 on the other hand, the IOP was elevated >50 mm Hg.

Cupping of the optic nerve head developed during the 30-day observation period in all treated eyes (Table 2, Figs. 2, 3). The cup to disc (C/D) ratios of monkeys #1 and #4 were increased from 0.2 and 0.3 to 0.4 and 0.7, respectively, during the follow-up period. In the monkeys with the higher IOP, the C/D ratio of the laser-treated eyes increased to 0.9 during the follow-up period (monkeys #2 and #3; Table 2).

The longitudinal sections of the optic disc from the left eyes (control eyes) of monkey #3 and #4 showed normal cup size of the disc and the lamina cribrosa (Fig. 3A). In the right eye of monkey #4, a slight backward bowing of the lamina cribrosa and some enlargement of cupping were observed (Fig. 3B). In the right eye of monkey #3, the lamina cribrosa was further bowed posteriorly and the cupping was more enlarged (Fig. 3C). Judging from the IOP and the enlargement of the optic disc cupping, the right eye of monkey #1 and the right eye of monkey #4 were diagnosed as having mild glaucoma and the right eye of monkey #2 and the right eye of monkey #3 severe glaucoma, although such a classification is rather arbitrary and severity of glaucoma is a continuum rather than separate entities.

Gene Microarray Analysis

The expression of several genes was upregulated and that of others was downregulated (Table 3). Genes that showed a change of expression greater than 1.7-fold in at least one of the pairwise probe comparisons were interpreted as showing a positive change. The number of upregulated genes excluding the ESTs was 45 and 18 in the retina of the right eye of monkey #1 (mild glaucoma) and the right eye of monkey #2 (severe glaucoma). The number of downregulated genes was 17 and 21 in the retina of the right eye of monkey #1 and monkey #2. Thus, only 0.7% of all the genes examined showed significant changes in mRNA expression in this experimental model of glaucoma.

The genes that showed an up- or downregulation in both mild and severe glaucoma retinas are listed on a gray background in Tables 3 and 4. For example, chitinase 3-like 1 gene, complement component 4A gene, B-factor gene, and *HLADR* α gene were upregulated in the right eye of both monkey #1 (mild glaucoma) and monkey #2 (severe glaucoma). The expression of v-akt murine thymoma viral oncogene homolog 1 gene was decreased in both specimens.

Although a relatively small number of genes was up- or downregulated in this experimental glaucoma model, some genes showed relatively large expression changes. For example, in the eyes with severe glaucoma, the expression of *GFAP* and ceruloplasmin was upregulated by 2.9- and 1.9-fold of the control level. The expression of neurofilament and parvalbumin in severe glaucoma decreased 3.0- and 1.8-fold of the control retina, respectively.

Scatter plots of the Cy3 fluorescence and Cy5 fluorescence in mild and severe glaucoma are shown in Figure 4. In both eyes, the two fluorescent intensities showed high coefficients but there were several genes that were located out of the regression lines. Among them, special attention was paid to *GFAP* and ceruloplasmin because their expression has also been reported to change in other experimental glaucoma models.[26,27]

Real-Time PCR Analysis

To validate microarray data, real-time PCR analysis of mRNA expression changes was performed on four genes that showed an up- or downregulation by the microarray analysis. The expression levels obtained by the analysis (monkey #2, right eye) were normalized to that of *β-actin* and were shown as the

TABLE 2. Characteristics of Experimental and Control Eyes

Monkey Eye	Diagnosis	Total Laser Energy (J)	Range of IOP (mm Hg)	Mean of IOP (mm Hg)	Followup (d)	Cup to Disk Ratio Initial	Cup to Disk Ratio Final
#1							
R	Mild glaucoma	48	11–44	36	30	0.2	0.4
L	Normal	0	22–24	22	—	0.3	0.3
#2							
R	Severe glaucoma	69	21–61	55	30	0.2	0.9
L	Normal	0	22–24	23	—	0.3	0.3
#3							
R	Severe glaucoma	43	21–68	57	30	0.2	0.9
L	Normal	0	22–24	23	—	0.2	0.2
#4							
R	Mild glaucoma	38	19–38	33	30	0.3	0.7
L	Normal	0	20–23	22	—	0.3	0.3

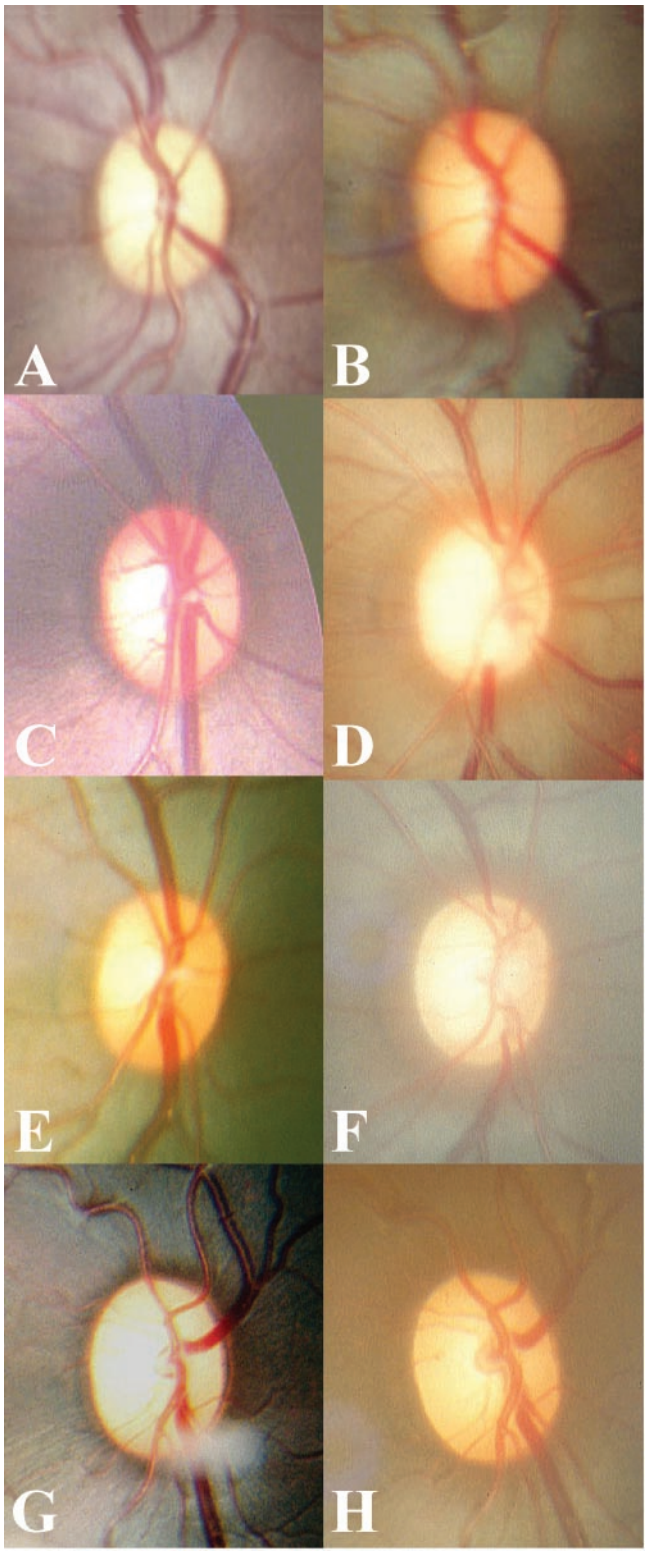

FIGURE 2. Optic disks before and after the laser treatment of the trabecular meshwork. Fundus photographs: the *left lane* (**A**, **C**, **E**, **G**) shows normal optic disks before the treatment, and the *right lane* (**B**, **D**, **F**, **H**) shows glaucomatous optic disks after laser application. (**A**) and (**B**) are from monkey #1, (**C**) and (**D**) are from monkey #2, (**E**) and (**F**) are from monkey #3, and (**G**) and (**H**) are from monkey #4.

fold increase or decrease relative to that of the control (monkey #2, left eye). The mRNA expression of ceruloplasmin was 2.85 ± 0.13-fold (mean ± SEM, $n = 6$) of the control retina; GFAP expression was increased to 8.09 ± 0.07-fold ($n = 6$) and that of chitinase 3-like 1 was upregulated to 3.91 ± 0.21-fold ($n = 6$). On the other hand, mRNA expression of *akt-1* decreased 1.74 ± 0.15-fold ($n = 6$) of the control retina. Thus real-time PCR analysis showed a similar pattern of mRNA expression changes in glaucomatous retina as shown by the microarray analysis.

Immunohistochemistry

Glial Fibrillary Acidic Protein. To confirm the upregulation and to determine the localization of GFAP protein expression in glaucomatous retinas, immunohistochemical studies were carried out on the eye with severe glaucoma (monkey #3, right eye) and mild glaucoma (monkey #4, right eye) and the control (monkeys #1, #3, and #4, left eye). In the eye with severe and mild glaucoma, immunoreactivities against GFAP were observed in the inner retina (nerve fiber layer and ganglion cell layer). There was a radial staining pattern suggesting the expression of GFAP in the Müller cells. The immunoreactivities of the severe glaucoma retina were stronger than those of mild glaucoma (Figs. 5A, 5B). In the control retina, only very weak immunoreactivities against GFAP were found (Fig. 5C).

Ceruloplasmin. In the retina with severe glaucoma (monkey #3, right eye), strong immunoreactivities against ceruloplasmin were observed in the internal limiting membrane, nerve fiber layer, ganglion cell layer, and inner nuclear layer, and a relatively weak radial pattern of the immunoreactivities were found in the outer plexiform layer and outer nuclear layer

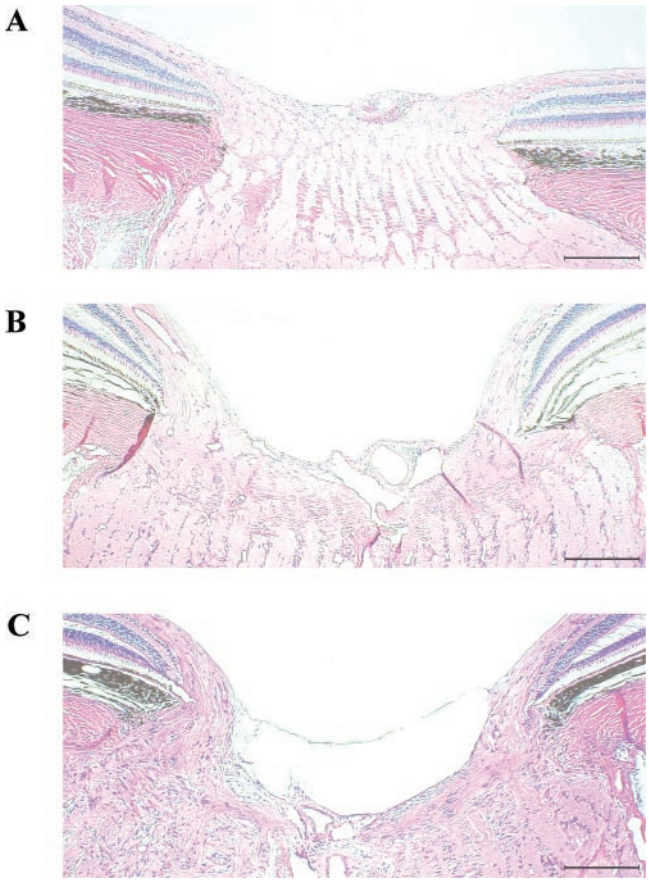

FIGURE 3. Longitudinal sections of the optic disc. (**A**) control (monkey #4, left eye); (**B**), mild glaucoma (monkey #4, right eye); (**C**), severe glaucoma (monkey #3, right eye). Backward bowing of the lamina cribrosa is evident in glaucomatous eyes (**B** and **C**). Hematoxylin-eosin staining. Scale bar, 250 μm.

TABLE 3. List of Up- or Downregulated Genes in Mild Glaucoma Retina

Accession No.	Gene Name	Fold of Change
	Cytoskeleton	
AI571257	bassoon (presynaptic cytomatrix protein)	1.7
M77016	tropomodulin	1.7
AW951177	myosin, light polypeptide kinase	−1.8
AB020673	myosin, heavy polypeptide 11, smooth muscle	−1.9
	Signal transduction	
S82807	Thyrotropin receptor {3′ region}	1.8
D21209	APO-1/CD95 (Fas)-associated phosphatase	1.8
U50648	protein kinase, interferon-inducible double stranded RNA dependent	1.8
U08471	folate receptor 3 (gamma)	1.7
AI313436	Fn14 for type 1 transmenmbrane protein	1.7
AI828515	tumor necrosis factor (ligand) superfamily, member 13	1.7
AI565773	v-erb-b2 avian erythroblastic leukemia viral oncogene homolog 3	1.7
NM_001547	interferon-induced protein 54	1.7
U96781	ATPase, Ca++ transporting, cardiac muscle, fast twitch 1	−1.7
AI597912	v-akt murine thymoma viral oncogene homolog 1	−2.0
	Remodelling	
AL035797	chitinase 3-like 1	1.9
AI347985	matrix metalloproteinase 23B	1.8
X07820	matrix metalloproteinase 10 (stromelysin 2)	1.7
AJ001531	protease, serine, 12 (neurotrypsin, motopsin)	1.7
	Transcription factor	
AL110195	microphthalmia-associated transcription factor	2.2
Z29678	microphthalmia-associated transcription factor	2
AK001893	target of myb1 (chicken) homolog-like 1	1.8
NM_005612	RE1-silencing transcription factor	1.7
D88827	zinc finger protein 263	1.7
AA451817	cyclin H	−1.7
NM_006475	osteoblast specific factor 2	−1.7
NM_002145	homeo box B2	−1.8
	Immune response	
AW404507	immunoglobulin kappa variable 1D-8	3.4
AA290845	immunoglobulin heavy constant α 1	2.4
AA613978	complement component 4A	2.3
BE244440	major histocompatibility complex, class I DR α	1.9
X72875	B-factor propendin	1.9
X03066	major histocompatibility complex, class II, DO β	1.7
AI652705	interleukin 16 (lymphocyte chemoaltractant factor)	1.7
	Others	
D63479	diacylglycerol kinase, delta (130kD)	2.3
AB007042	exostoses (multiple)-like 3	2.1
AI922381	KIAA0805 protein	2
AA402981	Homo sapiens clone 24775 mRNA sequence	2
AF052174	Homo sapiens clone 24630 mRNA sequence	1.8
AB014533	KIAA0633 protein	1.8
Z19585	thrombospondin 4	1.7
X76180	sodium channel, nonvoltage-gated 1 α	1.7
AW898081	SMA3	1.7
AI190043	hypothetical protein FLJ10925	1.7
NM_003007	semenogelin I	1.7
AW966003	eukaryotic translation elongation factor 1 α 1	1.7
AA534418	hypothetical protein FLJ20727	1.7
AI309555	hypothetical protein FLJ10913	1.7
AI608986	mesangium predominant gene, megsin	1.7
R55801	Homo sapiens cDNA FLJ20148 fis	1.7
W73858	microsomal glutathione S-transferase 2	1.7
AA112281	hypothetical protein FLJ20446	1.7
U09860	protease, serine, 7 (enterokinase)	1.7
U12595	heat shock protein 75	−1.7
NM_004566	6-phosphofrueto-2-kinase/fructose-2,6-biphosphatase 3	−1.7
BE314741	N-ethylmaleimide sensitive factor attachment protein, α	−1.7
X95735	zyxin	−1.7
M16652	elastase 1, pancreatic	−1.7
Y13618	ubiquitin specific protease 9, Y chromosome (Drosophila fat facets related)	−1.7
NM_000122	excision repair cross-complementing rodent repair deficiency, complementation group	−1.7
AF053356	postmeiotic segregation increased 2-like 12	−1.7
AF038007	familial intrahepatic cholestasis 1, (progressive, Byler disease and benign recurrent)	−1.7
NM_000189	hexokinase 2	−1.8

Genes that showed an up- or downregulation in both mild and severe glaucoma retinas are shown on a gray background.

TABLE 4. List of Up- or Downregulated Genes in Severe Glaucoma Retina

Accession No.	Gene Name	Fold of Change
	Cytoskeleton	
AL120727	ARP1 (actin-related protein 1, yeast) homolog A (centractin α)	−1.7
U38291	microtubule-associated protein 1A	−1.7
AB020652	neurofilament, heavy polypeptide (200kD)	−3.0
	Signal transduction	
BE396794	adrenergic, β, receptor kinase 1	1.9
AK000081	cell division cycle 2-like 1 (PITSLRE proteins)	−1.7
M82919	gamma-aminobutyric acid (GABA) A receptor, β 3	−1.7
Y08417	cholinergic receptor, nicotinic, beta polypeptide 3	−1.8
AI597912	v-akt murine thymonia viral oncogene homolog 1	−1.9
AL035250	endothelin 3	−2.1
	Remodelling	
AL035737	chitinase 3-like 1	1.9
MI8963	regenerating islet-derived 1 α	1.8
	Transcription factor	
AI885769	v-jun avian sarcoma virus 17 oncogene homolog	1.7
X78710	metal-regulatory transcription factor 1	−1.9
	Immune response	
AA613978	complement component 4A	3.1
X72875	B-factor, properdin	2.2
K02765	complement component 3	1.9
BE244440	major histocompatibility complex, class II, DR α	1.9
M13560	CD74 antigen	1.8
M18044	complement component receptor 3, α, CD11b (p170)	1.8
AI554230	complement component 1, q subcomponent, β polypeptide	1.8
L05424	CD44 antigen (homing function and Indian blood group system)	1.7
AF178980	B-cell associated protein	1.7
	Others	
AA059335	glial fibrillary acidic protein (GFAP)	2.9
AW950668	ceruloplasmin (ferroxidase)	1.9
AF089747	α-1-antichymotrypsin	1.8
AI922381	KIAA0805 protein	1.8
AA402981	Homo sapiens clone 24775 mRNA sequence	1.7
NM_000755	carnitine acetyltransferase	−1.7
AB014606	KIAA0706 gene product	−1.7
AL137297	KIAA0842 protein	−1.7
AB007877	KIAA0417 gene product	−1.7
AL117401	DKFZp434P211 protein	−1.7
BE314741	N-ethylmaleimide-sensitive factor attachment protein, α	−1.7
D84107	RNA-binding protein gene with multiple splicing	−1.7
M57736	phosphodiesterase I/nucleotide pyrophosphatase 1	−1.7
AI022812	parvalbumin	−1.8
X52941	lactotransferrin	−1.9
AI928978	ubiquitin carboxyl-terminal esterase L1 (ubiquitin thiolesterase)	−1.9
DI3643	KIAA0018 gene product	−1.9

Genes that showed an up- or downregulation in both mild and severe glaucoma retinas are shown on a gray background.

(Fig. 5E). In the retina with mild glaucoma (monkey #4, right eye), strong immunoreactivities against ceruloplasmin were observed in the internal limiting membrane, nerve fiber layer, and the ganglion cell layer, but the immunoreactivity of the inner nuclear layer was much weaker compared with that of severe glaucoma retina (Fig. 5F). There were also strong ceruloplasmin-like immunoreactivities in the vitrous of both severe and mild glaucoma (Figs. 5I, 5J). In the control retina, very weak ceruloplasmin-like immunoreactivities were found in the inner retina but no immunoreactivity was found in the vitreous (Figs. 5G, 5K).

Double Staining of GFAP and Ceruloplasmin. To determine differences in the expression patterns of GFAP and ceruloplasmin, double immunostaining was performed on the section of the retina with severe glaucoma. GFAP and ceruloplasmin were coexpressed in Müller cells, but their distribution patterns were not completely the same (Fig. 6). GFAP-like immunoreactivities were seen in cells that were located in the inner most layer of the retina, but the ceruloplasmin-like immunoreactivities were not found in such cells. Most likely, astrocytes express GFAP but they do not express ceruloplasmin. Interestingly, ceruloplasmin-like immunoreactivities were

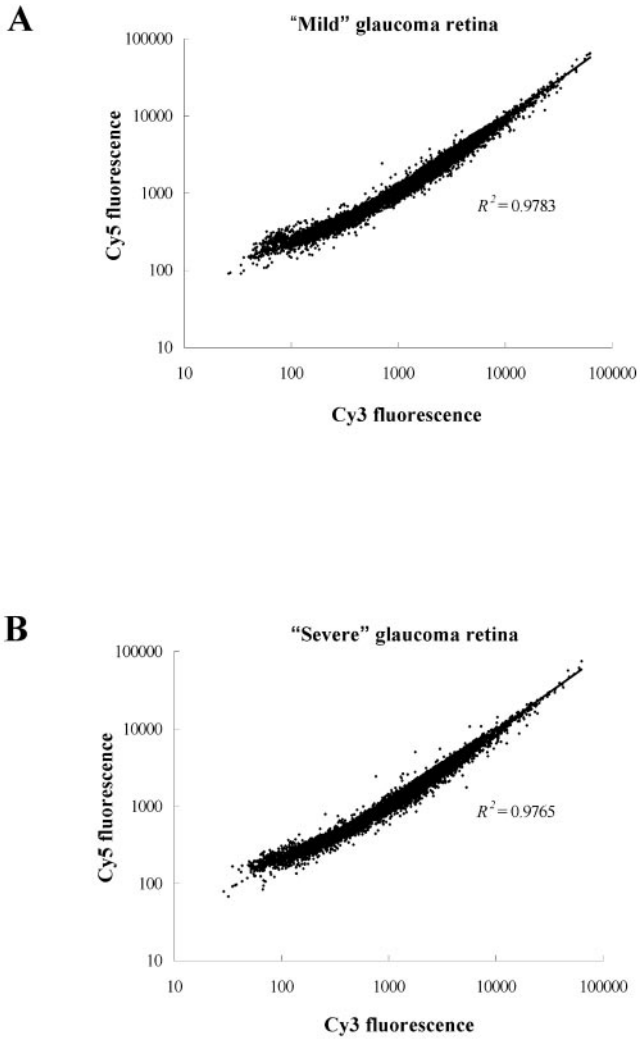

FIGURE 4. Scatter plot of gene expression changes. Scatter plots (on logarithmic axes) of the gene expression ratios for all array elements with linear regression lines fitted to the data. R^2 is the coefficient of determination. (**A**) Monkey #1, right eye (mild glaucoma). (**B**) Monkey #2, right eye (severe glaucoma).

also found in the internal limiting membrane and in the vitreous body (Fig. 6).

Akt, Neurofilament and Parvalbumin. Immunohistochemical studies on akt, neurofilament, and parvalbumin protein expression were carried out. The immunoreactivities against akt were observed ubiquitously in all specimens. The immunoreactivities against neurofilament were obserbed in the nerve fiber layer and some cells in the ganglion cell layer in all specimens. The immunoreactivities against parvalbumin were observed in some cells in the ganglion cell layer and the internal nuclear layer in all specimens. But the strength of immunostainings against akt, neurofilament, and parvalbumin gene products was not different among the specimens studied (graphic data not shown).

DISCUSSION

The primate model of laser-induced glaucoma closely resembles human glaucoma.[15,16] Human microarray chips, instead of monkey chips, were used in this study because ready-made chips for monkeys were not available. Because of the high homology in the genes of the two species,[28,29] the use of a human chip on monkey tissues is usually acceptable, though there may be some important genes that may not be detected in the analysis.[30] It has been reported that the mean identity between monkey and human cDNA is approximately 95%.[28] A study of the sensitivity and specificity of oligonucleotide microarrays has demonstrated that sequences with greater than 75–80% identity will cross-hybridize and contribute to the overall signal.[31]

Among the 9182 genes examined, only 0.7% were found to be up- or downregulated in this monkey glaucoma model. Compared with human glaucoma, the death of the RGC in the monkey retina is rapid, but even so, the process is much slower than other models of retinal neuronal apoptosis such as the retinal ischemia-reperfusion injury or retinal light damage. This may explain why only modest expression changes were detected by the microarray analysis and only 0.7% of the genes examined showed significant up- or downregulation. It is also noteworthy that only a limited number of genes that have been shown to play a role in neuronal apoptosis demonstrated changes in expression. For example, the caspases, immediate early genes, and *Bcl-2* family genes including *Bax*, which have been shown to be involved in the apoptosis cascade, did not show significant expression changes in the monkey glaucomatous eyes. However, it should be noted that in the monkey model of laser-induced glaucoma, only 1% of retinal ganglion cells are known to be TUNEL-positive.[3] These data may explain why only a limited number of genes involved with neuronal apoptosis showed expression changes.

Even so, *akt* was downregulated in both the mild and severe glaucomatous retinas by the microarray analysis. The real-time PCR analysis confirmed the downregulation. Although ubiquitously expressed in various cells, the downregulation of anti-apoptotic genes such as *akt* may be important in the process of RGC apoptosis. The TNF superfamily, member 13 (APRIL/TRDL-1),[32] is another example of a gene that seems to play a role in retinal neuronal apoptosis, and was found to be upregulated in the retina with mild glaucoma. This protein has a function similar to TNF-α in that APRIL binds with TNF-α receptor-1.[32] TNF-α receptor-1 is present on RGCs, and RGCs are sensitive to the cytotoxic effects of TNF-α. The increased production of TNF-α by glial cells in glaucomatous eyes may participate in the death of RGCs through direct activation of the apoptotic cell death cascade.[33] Moreover, there is a report which suggests a possible interaction between HLA-DR, NOS-2 and TNF-α.[34]

Genes that may play a role in the remodeling of retinal structure showed some upregulation in this glaucoma model. For example, matrix metalloproteinase 23B and 10 were upregulated in the mild glaucoma retina, and chitinase 3-like 1 (YKL-40, hc-gp 39)[35,36] was also upregulated in both the mild and severe glaucomatous retinas. Thus, it is reasonable to consider that these genes are involved in tissue remodeling after the glaucomatous damage.

Immunorelated genes, such as *HLA-DR* α, *HLA-DO* β, complement component 1, complement component 3, and complement component receptor 3α were also upregulated. HLA-DR is a microglial marker, and it has been reported that the number of microglial cells was increased in a glaucoma model, and that activated microglial cells have been identified in human glaucomatous eyes[37] (Tezel G. *IOVS* 2002;43:ARVO E-Abstract 2182). Neurofilament, heavy polypeptide (200 kDa), parvalbumin, microtubule-associated protein 1A, γ-aminobutyric acid A receptor, type β3, and nicotinic receptor were downregulated. Neurofilament and parvalbumin immunoreactivities have been shown in a subpopulation of RGCs (especially large cells), and neurofilament immunoreactive cells represented a large proportion of the cells that degenerated in the monkey experimental glaucoma eyes.[38] The data suggested that a reduction in the number of retinal ganglion cells could be shown at the mRNA level.

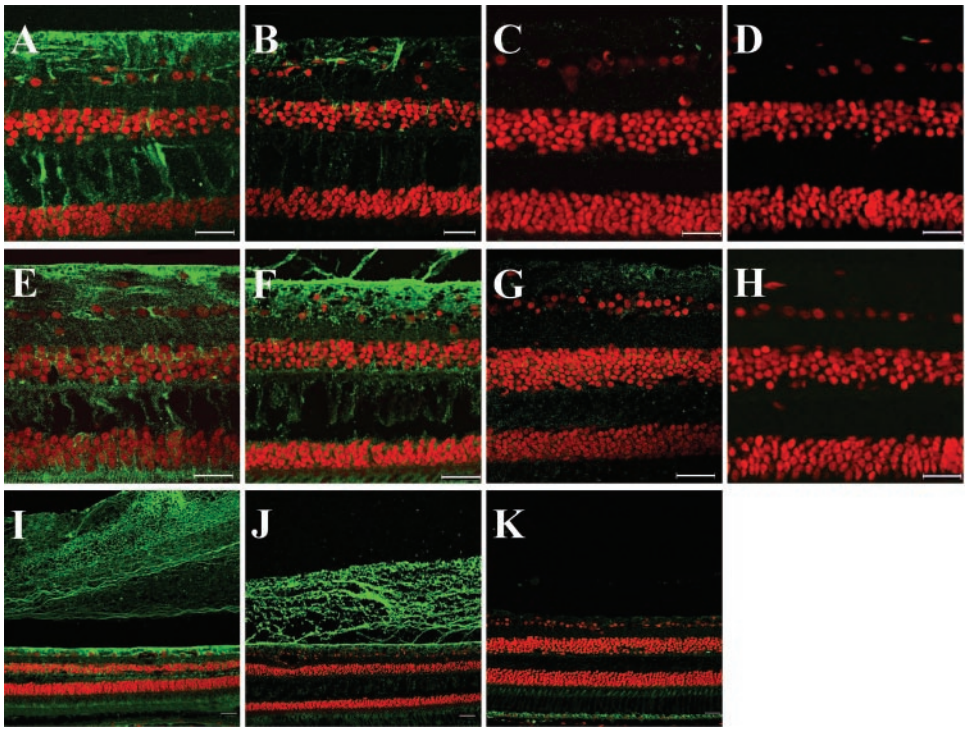

FIGURE 5. Immunohistochemical studies for GFAP and ceruloplasmin. Severe glaucoma retina from monkey #3, right eye (**A**, **D**, **E**, **H**, **I**), mild glaucoma retina from monkey #4, right eye (**B**, **F**, **J**), and control retina from monkey #4, left eye (**C**, **G**, **K**) were stained with anti-GFAP antibody and anticeruloplasmin antibody. *Green* represents GFAP-like immunoreactivities (**A–D**) and ceruloplasmin-like immunoreactivities (**E–K**). (**D**) and (**H**) are negative controls with no primary antibody of GFAP and ceruloplasmin. *Red* represents nuclear staining by propidium iodide. GCL, ganglion cell layer; INL, inner nuclear layer; ONL, outer nuclear layer. Scale bar, 25 μm.

The major drawback of this study is that only a small number of animals were used and thus it was not possible to determine whether the changes in gene expression profile really represent glaucomatous retinal damage or are just differences in individual animals. Another drawback is that replication of microarray experiments was not done. However, the age, body weight, and gender as well as handling and feeding of the monkeys were constant. Furthermore, as shown in Figure 4, the coefficients of determination of gene expression between the control and glaucomatous retina were very high. These facts may support the idea that the gene expression changes found in this study really represent the effect of glaucomatous retinal damage. It cannot easily be explained why some genes that showed up- or downregulation in mild glaucoma did not show significant expression changes in severe glaucoma. One possible explanation is that glaucomatous retinal damage is not a state but a process in which different genes play different roles during the process. In spite of the above drawbacks, we believe the data presented in this study is meaningful because the real-time PCR analysis supported the microarray data, though a limited number of gene expression was studied by the analysis. The real-time PCR analysis also compensates for the lack of repetition of the microarray analysis.

Our immunohistochemical studies demonstrated expression of GFAP in Müller cells and astrocytes of the glaucomatous retinas. GFAP is known to be expressed in Müller cells after ocular injury,[39,40] and Müller cells are thought to play a central role in the homeostatic regulation of the retina.[41,42] Increased expression of GFAP in Müller cells and astrocytes may be explained by disturbed homeostasis in the experimental glaucoma eyes. Ceruloplasmin was also found to be expressed in Müller cells and vitreous (Figs. 5E, 6). The immunostatining of vitreous, internal limiting membrane, and ganglion cell layer against ceruloplasmin was observed both in severe and mild glaucomatous retina. But the immunostaining of the inner nuclear layer considered to be the nucleus of Müller cells was observed only in the severe glaucoma, not in the mild glaucoma. Also in the microarray analysis, ceruloplasmin was upregulated in the severe glaucoma but not in the mild glaucoma.

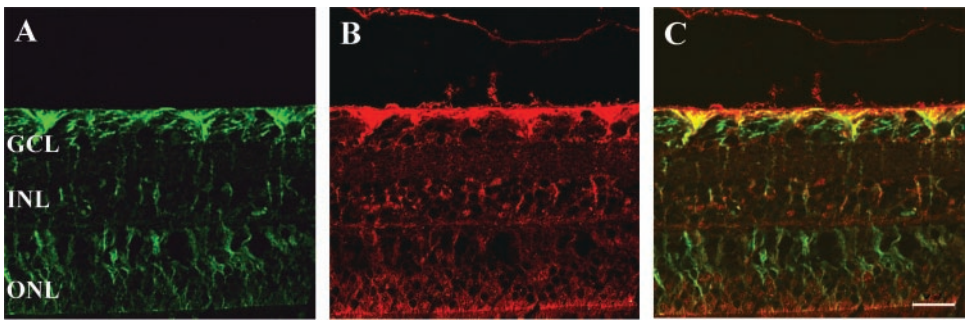

FIGURE 6. Double immunostaining for GFAP and ceruloplasmin. Sections from severe glaucoma retina from monkey #3, right eye, were (**A**) double stained by anti-GFAP antibody (*green*) and (**B**) anticeruloplasmin antibody (*red*). GFAP-like immunoreactivity was found in Müller cells and astrocytes whereas ceruloplasmin-like immunoreactivity was found in the internal limiting membrane and Müller cells. (**C**) Merged image of GFAP and ceruloplasmin. GCL, ganglion cell layer; INL, inner nuclear layer; ONL, outer nuclear layer. Scale bar, 25 μm.

These results suggest that there may be two origins of ceruloplasmin. One of the two origins can be plasma protein from the break down of the blood-ocular barrier.[43] The other origin seems to be Müller cells.[27,44] Ceruloplasmin has endogenous scavenger and ferroxidase activities.[45,46] Upregulated ceruloplasmin may inhibit formation of reactive oxygen species and block lipid peroxidation.[47] Lipid peroxidation is considered to play a role in neuronal cell death.[24] So, increased ceruloplasmin may act as an endogenous scavenger and may prevent apoptotic cell death. It has been reported that the expression of ceruloplasmin is upregulated in the optic nerve transection model and the retinal light damage model in the rat[48] (Kageyama M. *IOVS* 2001;42:ARVO Abstract 2210; Farkas RH. *IOVS* 2003;44:ARVO Abstract 4390). There have been several recent reports on human subjects with aceruloplasminemia, in whom mutations in the ceruloplasmin gene prevented the expression of the native protein. These patients were reported to have retinal degeneration.[49–51] Upregulated expression of ceruloplasmin in Müller cells and vitreous may play a role as an endogenous scavenger against reactive oxygen species. It may be a rational explanation that the production of ceruloplasmin in Müller cells increases to maintain the homeostasis in the retina only when the degeneration or death of RGC disturbs the intraocular environment to some extent.

In summary, we showed the gene expression profiling in the retina of the laser-induced monkey glaucoma model at 30 days after the laser treatment. In our analysis only a very limited number of genes showed up- or downregulation. The possible roles of such genes should be studied further in detail in the near future.

References

1. Quigley HA. Number of people with glaucoma worldwide. *Br J Ophthalmol.* 1996;80:389–393.
2. Garcia-Valenzuela E, Shareef S, Walsh J, Sharma SC. Programmed cell death of retinal ganglion cells during experimental glaucoma. *Exp Eye Res*. 1995;61:33–44.
3. Quigley HA, Nickells RW, Kerrigan LA, Pease ME, Thibault DJ, Zack, DJ. Retinal ganglion cell death in experimental glaucoma and after axotomy occurs by apoptosis. *Invest Ophthalmol Vis Sci*. 1995;36:774–786.
4. Anderson DR, Hendrickson A. Effect of intraocular pressure on rapid axoplasmic transport in monkey optic nerve. *Invest Ophthalmol Vis Sci*. 1974;13:771–783.
5. Quigley HA, Addicks EM, Green WR, Maumenee AE. Optic nerve damage in human glaucoma. II. The site of injury and susceptibility to damage. *Arch Ophthalmol*. 1981;99:635–649.
6. Quigley HA, Anderson DR. The dynamics and location of axonal transport blockade by acute intraocular pressure elevation in primate optic nerve. *Invest Ophthalmol Vis Sci*. 1976;15:606–616.
7. Dreyer EB, Zurakowski D, Schumer RA, Podos SM, Lipton SA. Elevated glutamate levels in the vitreous body of humans and monkeys with glaucoma. *Arch Ophthalmol*. 1996;114:299–305.
8. Neufeld AH, Hernandez MR, Gonzalez M. Nitric oxide synthase in the human glaucomatous optic nerve head. *Arch Ophthalmol*. 1997;115:497–503.
9. Liu B, Neufeld AH. Expression of nitric oxide synthase-2 (NOS-2) in reactive astrocytes of the human glaucomatous optic nerve head. *Glia*. 2000;30:178–186.
10. Williams GT, Smith CA. Molecular regulation of apoptosis: genetic controls on cell death. *Cell*. 1993;74:777–779.
11. Johnson EC, Morrison JC, Farrell S, et al. The effect of chronically elevated intraocular pressure on the rat optic nerve head extracellular matrix. *Exp Eye Res*. 1996;62:663–674.
12. Morrison JC, Moore CG, Deppmeier LM, et al. A rat model of chronic pressure induced optic nerve damage. *Exp Eye Res*. 1997; 64:85–96.
13. Shareef SR, Garcia-Valenzuela E, Salierno A, Walsh J, Sharma SC. Chronic ocular hypertension following episcleral venous occlusion in rats. *Exp Eye Res*. 1995;61:379–382.
14. Ueda J, Sawaguchi S, Hanyu T, et al. Experimental glaucoma model in the rat induced by laser trabecular photocoagulation after an intracameral injection of Indian ink. *Jpn J Ophthalmol*. 1998;42: 337–344.
15. Gaasterland D, Kupfer C. Experimental glaucoma in the rhesus monkey. *Invest Ophthalmol Vis Sci*. 1974;13:455–457.
16. Pederson JE, Gaasterland DE. Laser-induced primate glaucoma. I. Progression of cupping. *Arch Ophthalmol*. 1984;102:1689–1692.
17. Iyer VR, Eisen MB, Ross DT, et al. The transcriptional program in the response of human fibroblasts to serum. *Science*. 1999;283: 83–87.
18. Duggan DJ, Bittner M, Chen Y, Meltzer P, Trent JM. Expression profiling using cDNA microarrays. *Nat Genet*. 1999;21:10–14.
19. Brown PO, Botstein D. Exploring the new world of the genome with DNA microarrays. *Nat Genet*. 1999;21:33–37.
20. Southern E, Mir K, Shchepinov M. Molecular interactions on microarrays. *Nat Genet*. 1999;21:5–9.
21. Sawaguchi S, Yue BY, Fukuchi T, et al. Collagen fibrillar network in the optic nerve head of normal monkey eyes and monkey eyes with laser-induced glaucoma—a scanning electron microscopic study. *Curr Eye Res*. 1999;18:143–149.
22. Fukuchi T, Sawaguchi S, Yue BY, Iwata K, Hara H, Kaiya T. Sulfated proteoglycans in the lamina cribrosa of normal monkey eyes and monkey eyes with laser-induced glaucoma. *Exp Eye Res*. 1994;58: 231–243.
23. Perkin–Elmer Applied Biosystems: *User Bulletin No. 2* (II December, 1997)
24. Shibuki H, Katai N, Yodoi J, Uchida K, Yoshimura N. Lipid peroxidation and peroxynitrite in retinal ischemia-reperfusion injury. *Invest Ophthalmol Vis Sci*. 2000;41:3607–3614.
25. Kuroiwa S, Katai N, Yoshimura N. A possible role for $p16^{INK4}$ in neuronal cell death after retinal ischemia-reperfusion injury. *Invest Ophthalmol Vis Sci*. 1999;40:528–533.
26. Tanihara H, Hangai M, Sawaguchi S, et al. Up-regulation of glial fibrillary acidic protein in the retina of primate eyes with experimental glaucoma. *Arch Ophthalmol*. 1997;115:752–756.
27. Levin LA, Geszvain KM. Expression of ceruloplasmin in the retina: induction after optic nerve crush. *Invest Ophthalmol Vis Sci*. 1998;39:157–163.
28. Zou J, Young S, Zhu F, et al. Microarray profile of differentially expressed genes in a monkey model of allergic asthma. *Genome Biol.* 2002;3:research0020.
29. Osada N, Hida M, Kusuda J, Tanuma R, Iseki K. Assignment of 118 novel cDNAs of cynomolgus monkey brain to human chromosomes. *Gene*. 2001;275:31–37.
30. Bigger CB, Brasky KM, Lanford RE. DNA microarray analysis of chimpanzee liver during acute resolving hepatitis C virus infection. *J Virol*. 2001;75:7059–7066.
31. Kane MD, Jatkoe TA, Stumpf CR, et al. Assessment of the sensitivity and specificity of oligonucleotide (50mer) microarrays. *Nucleic Acids Res*. 2000;28:4552–4557.
32. Kelly K, Manos E, Jensen G, Nadauld L, Jones DA. APRIL/TRDL-1, a tumor necrosis factor-like ligand, stimulates cell death. *Cancer Res*. 2000;60:1021–1027.
33. Tezel G, Li LY, Patil RV, Wax MB. TNF-alpha and TNF-alpha receptor-1 in the retina of normal and glaucomatous eyes. *Invest Ophthalmol Vis Sci*. 2001;42:1787–1794.
34. Yuan L, Neufeld AH. Tumor necrosis factor-alpha: a potentially neurodestructive cytokine produced by glia in the human glaucomatous optic nerve head. *Glia*. 2000;32:42–50.
35. Recklies AD, White C, Ling H. The chitinase 3-like protein human cartilage glycoprotein 39 ($HC\text{-}gp^{39}$) stimulates proliferation of human connective-tissue cells and activates both extracellular signal-regulated kinase- and protein kinase B-mediated signalling pathways. *Biochem J*. 2002;365:119–126.
36. Tsuji T, Matsuyama Y, Natsume N, et el. Analysis of chondrex (YKL-40, HC gp-39) in the cerebrospinal fluid of patients with spine disease. *Spine.* 2002;27:732–735.
37. Yang J, Yang P, Tezel G, et al. Induction of HLA-DR expression in human lamina cribrosa astrocytes by cytokines and simulated ischemia. *Invest Ophthalmol Vis Sci*. 2001;42:365–371.

38. Vickers JC, Schumer RA, Podos SM, Wang RF, Riederer BM, Morrison JH. Differential vulnerability of neurochemically identified subpopulations of retinal neurons in a monkey model of glaucoma. *Brain Res*. 1995;680:23–35.
39. Grosche J, Hartig W, Reichenbach A. Expression of glial fibrillary acidic protein (GFAP), glutamine synthetase (GS), and Bcl-2 protooncogene protein by Müller (glial) cells in retinal light damage of rats. *Neurosci Lett*. 1995;185:119–122.
40. Osborne NN, Block F, Sontag KH. Reduction of ocular blood flow results in glial fibrillary acidic protein (GFAP) expression in rat retinal Müller cells. *Vis Neurosci*. 1991;7:637–639.
41. Newman E, Reichenbach A. The Müller cell: a functional element of the retina. *Trends Neurosci*. 1996;19:307–312.
42. Bringmann A, Reichenbach A. Role of Müller cells in retinal degenerations. *Front Biosci*. 2001;6:E72–E92.
43. McGahan MC, Fleisher LN. Antioxidant activity of aqueous and vitreous humor from the inflamed rabbit eye. *Curr Eye Res*. 1986; 5:641–645.
44. Klomp LW, Gitlin JD., Expression of the ceruloplasmin gene in the human retina and brain: implications for a pathogenic model in aceruloplasminemia. *Hum Mol Genet*. 1996;5:1989–1996.
45. Loeffler DA, LeWitt PA, Juneau PL, et al. Increased regional brain concentrations of ceruloplasmin in neurodegenerative disorders. *Brain Res*. 1996;738:265–274.
46. Loeffler DA, DeMaggio AJ, Juneau PL, et al. Ceruloplasmin is increased in cerebrospinal fluid in Alzheimer's disease but not Parkinson's disease. *Alzheimer Dis Assoc Disord*. 1994;8:190–197.
47. Gutteridge JM. Antioxidant properties of caeruloplasmin towards iron- and copper dependent oxygen radical formation. *FEBS Lett*. 1983;157:37–40.
48. Chen L, Dentchev T, Wong R, et al. Increased expression of ceruloplasmin in the retina following photic injury. *Mol Vis*. 2003; 30:151–158.
49. Yoshida K, Furihata K, Takeda S, et al. A mutation in the ceruloplasmin gene is associated with systemic hemosiderosis in humans. *Nat Genet*. 1995;9:267–272.
50. Morita H, Ikeda S, Yamamoto K, et al. Hereditary ceruloplasmin deficiency with hemosiderosis: a clinicopathological study of a Japanese family. *Ann Neurol*. 1995;37:646–656.
51. Miyajima H, Nishimura Y, Mizoguchi K, et al. Familial apoceruloplasmin deficiency associated with blepharospasm and retinal degeneration. *Neurology*. 1987;37:761–767.